

The formaldehyde sensitivity of $\text{LaFe}_{1-x}\text{Zn}_x\text{O}_3$ -based gas sensor

Shanxing Huang · Hongwei Qin · Peng Song ·
Xing Liu · Lun Li · Rui Zhang · Jifan Hu ·
Hongdan Yan · Minhua Jiang

Received: 23 January 2007 / Accepted: 12 July 2007 / Published online: 22 September 2007
© Springer Science+Business Media, LLC 2007

Abstract Rare earth oxides $\text{LaFe}_{1-x}\text{Zn}_x\text{O}_3$ were synthesized by sol–gel method. The X-ray diffraction patterns (XRD) showed that $\text{LaFe}_{1-x}\text{Zn}_x\text{O}_3$ oxides are single phase with orthorhombic perovskite structure, they all show p-type semiconducting properties. Among nanocrystalline $\text{LaFe}_{1-x}\text{Zn}_x\text{O}_3$ oxides, $\text{LaFe}_{0.77}\text{Zn}_{0.23}\text{O}_3$ exhibits the highest sensitivity of 44.5 to 100 ppm formaldehyde. The optimal working temperature was found to be around 240 °C. Moreover the $\text{LaFe}_{0.77}\text{Zn}_{0.23}\text{O}_3$ exhibits short response and recovery time to 100 ppm formaldehyde. The lattice parameter doesn't agree with Vegard's law with the increasing Zn content, and the relative density was 70–80%.

Introduction

Formaldehyde (HCHO), an important chemical used widely by industry to manufacture building materials and numerous household products, is colorless and pungent-smelling, which can cause burning sensations in the eyes and throat, nausea, and difficult in breathing in some human exposed at elevated levels. Formaldehyde is considered as a major cause of sick building syndrome (SBS)

[1]. High concentrations of formaldehyde may even cause cancer in humans. Thus, it is significant to detect formaldehyde rapidly and accurately.

Recently perovskite compounds have attracted much attention due to their unique catalytic action [2], and gas-sensing properties [3–18]. The sensing behaviors of RFeO_3 (R = La, Nd, Sm, Gd, and Dy) for NO_2 and CO were found [7, 12]. However the resistances of RFeO_3 sensors are very high, which is a disadvantage in application. The replacement of rare earth element La by Ca, Sr, Ba and Pb in RFeO_3 can decrease the resistance. It has been found that $\text{La}_{0.68}\text{Pb}_{0.32}\text{FeO}_3$ shows good gas-sensing characteristics to formaldehyde gas. In this paper, nanocrystalline $\text{LaFe}_{1-x}\text{Zn}_x\text{O}_3$ ($x = 0.09, 0.16, 0.23$ and 0.3) were synthesized by sol–gel method. Results indicate that $\text{LaFe}_{1-x}\text{Zn}_x\text{O}_3$ ($x = 0.09, 0.16, 0.23$ and 0.3) oxides are single phase with orthorhombic perovskite structure. Zn-doping enhances the conductivity, gas sensitivity of LaFeO_3 .

Experimental

Preparation of $\text{LaFe}_{1-x}\text{Zn}_x\text{O}_3$ powders

The nanocrystalline $\text{LaFe}_{1-x}\text{Zn}_x\text{O}_3$ powders were prepared by the citric method: firstly we dissolved $\text{La}(\text{NO}_3)_3 \cdot 6\text{H}_2\text{O}$, $\text{Fe}(\text{NO}_3)_3 \cdot 9\text{H}_2\text{O}$, $\text{Zn}(\text{NO}_3)_2 \cdot 6\text{H}_2\text{O}$ and citric acid (all analytically pure) in ion-free water at 70 °C. Then polyethylene glycol (PEG molecular weight 20,000) was added under constant stirring to obtain sol and dried the sol into gel, then the gel pieces were ground to form a fine powder. For subsequent annealing, the samples were placed in an oven at 800 °C for 5 h. The power constituents were characterized by X-ray diffraction (XRD).

S. Huang · H. Qin (✉) · P. Song · X. Liu · L. Li · R. Zhang ·
J. Hu · M. Jiang
State Key Laboratory of Crystal Materials & Department of
Physics, Shandong University, Jinan 250100, P.R. China
e-mail: qin-hw@vip.163.com

H. Yan
Department of Physics, Kunming University of Science and
Technology, Kunming, P.R. China

Measurement of gas sensor

The prepared $\text{LaFe}_{1-x}\text{Zn}_x\text{O}_3$ powders were mixed with a polyvinyl acetate (PVA) solution and then ground into paste. Then, the paste was coated onto an Al_2O_3 tube on which two electrodes had been installed at each end. The Al_2O_3 tube was about 8 mm in length, 2 mm in outer diameter, and 1.6 mm in inner diameter. In order to improve their stability and repeatability, the gas sensors were calcined at 400 °C for 2 h.

The sensitivity S is defined as $S = R_{\text{HCHO}}/R_{\text{air}}$, where R_{HCHO} is the resistance measured under working circumstance, while R_{air} is the resistance value in the air. The sensor resistance was measured by a conventional circuit.

Results and discussion

Crystal structure of $\text{LaFe}_{1-x}\text{Zn}_x\text{O}_3$

XRD patterns of $\text{LaFe}_{1-x}\text{Zn}_x\text{O}_3$ powders are shown in Fig. 1. It is found that all the powders were perovskite phases with orthorhombic structure. The tolerance factor (t) is a quantitative measure of the structural perfection of the ABO_3 perovskite:

$$t = (r_A + r_O) / \sqrt{2}(r_B + r_O)$$

where r_A is the ionic radius of A cation, r_B the ionic radius of B cation and r_O is the ionic radius of oxygen. A mixture of Fe^{3+} (64.5 pm) and Zn^{2+} (74.5 pm) on the B-site could produce an average radius suitable for a perovskite

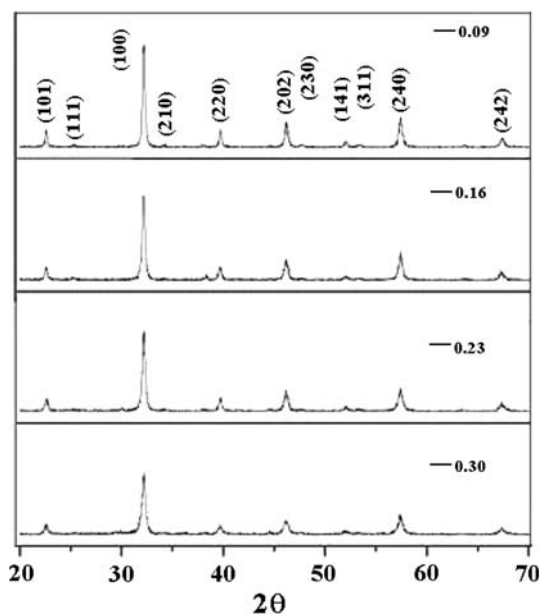


Fig. 1 The XRD pattern of $\text{LaFe}_{1-x}\text{Zn}_x\text{O}_3$ with $x = 0.09, 0.16, 0.23, 0.3$

Table 1 Lattice parameters of $\text{LaFe}_{1-x}\text{Zn}_x\text{O}_3$

| x value | Lattice constant (Å) | | | Volume |
|-----------|----------------------|--------|--------|---------|
| | a | b | c | |
| 0.09 | 5.5664 | 7.8592 | 5.5551 | 243.021 |
| 0.16 | 5.5675 | 7.8661 | 5.5562 | 243.331 |
| 0.23 | 5.5681 | 7.8684 | 5.5576 | 243.490 |
| 0.30 | 5.5672 | 7.8659 | 5.5561 | 243.307 |

structure with $t = 0.936, 0.933, 0.930$ and 0.927 when $x = 0.09, 0.16, 0.26$ and 0.3 , respectively. The lattice parameters of $\text{LaFe}_{1-x}\text{Zn}_x\text{O}_3$ are listed in Table 1. We can find that when $x = 0.3$, the unit cell parameter and volume becomes smaller. So we can say that the unit cell parameter doesn't agree with the Vegard's law. The phenomena can be explained by the formation of oxygen vacancies. When the Fe^{3+} ion is substituted by the Zn^{2+} ion at the B-site, in the view of charge compensation, oxygen vacancies are produced to maintain a neutral charge. The lattice might be somewhat smaller in order to maintain normal perovskite structure. Therefore, when $x = 0.3$, a large number of oxygen vacancies have been produced, which results in the unit cell volume becomes smaller.

In Table 2, the measured sintered density (d_s), the theoretical density (d_t), and the relative density ($d_s/d_t \times 100\%$) are given. The sintered density of $\text{LaFe}_{1-x}\text{Zn}_x\text{O}_3$ after sintering at 800 °C for 3 h was about 70–80% of the theoretical density.

Figure 2 shows the TEM image of the $\text{LaFe}_{0.77}\text{Zn}_{0.23}\text{O}_3$ powders prepared by sol–gel method after calcined at 800 °C for 2 h. The average grain size calculated in proportion to the photos is about 30 nm.

Figure 3 shows the statistical grain size distributions recorded in $\text{LaFe}_{0.77}\text{Zn}_{0.23}\text{O}_3$. One conclusion also may be reached from inspection of Fig. 3 that the average grain size, D is about 30 nm.

Electronic properties

Figure 4 depicts the resistance-temperature behavior of $\text{LaFe}_{1-x}\text{Zn}_x\text{O}_3$ -based sensor in air. In the whole temperature

Table 2 Measured sintered density, theoretical density and relative density of $\text{LaFe}_{1-x}\text{Zn}_x\text{O}_3$

| x value | Sintered density d_s (g/cm^3) | Theoretical density d_t (g/cm^3) | Relative density/(%) |
|-----------|--|---|----------------------|
| 0.09 | 3.7778 | 5.1751 | 73 |
| 0.16 | 3.8956 | 5.2432 | 74.3 |
| 0.23 | 4.3997 | 5.3656 | 82 |
| 0.30 | 4.201 | 5.5134 | 76.2 |

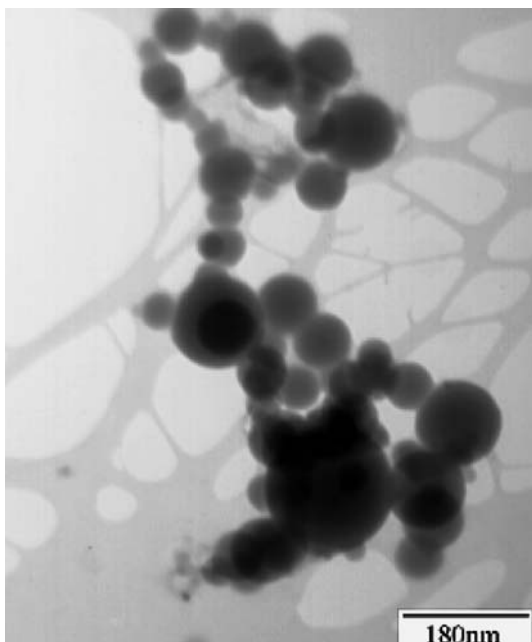
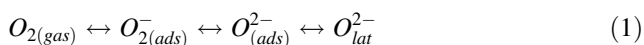


Fig. 2 TEM micrographs of $\text{LaFe}_{0.77}\text{Zn}_{0.23}\text{O}_3$ sintered at $800\text{ }^\circ\text{C}$ for 5 h

range, the resistance of all sensors decreases with increasing temperature, and that is the intrinsic characteristic of semiconductor. But no resistance peak occurs in the R – T curve with increasing temperature in air. This behavior is not similar to the typical surface controlled model [15]. With increasing temperature in air, the state of oxygen adsorbed on the surface of $\text{LaFe}_{1-x}\text{Zn}_x\text{O}_3$ undergoes the following reactions:



where the subscripts gas, ads and lat mean the state of gas, adsorption and lattice, respectively. The oxygen species capture electrons from the materials, leading to h^\cdot concentration increase. This is the reason why no resistance peak occurs.

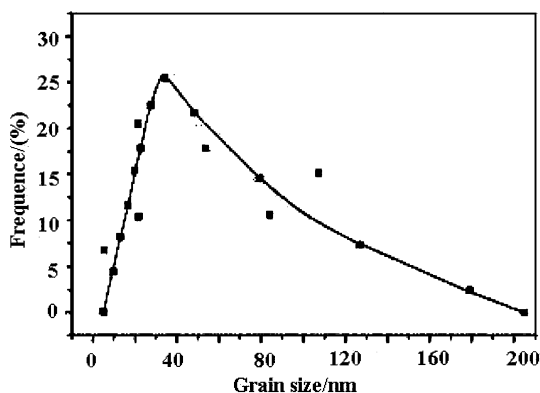


Fig. 3 The grain size distribution of $\text{LaZn}_{0.23}\text{Fe}_{0.77}\text{O}_3$

It is obviously from Fig. 4 that the Zn^{2+} doping enormously enhances the conductivity of the samples. $\text{LaFe}_{1-x}\text{Zn}_x\text{O}_3$ are all p-type semiconductive materials, and the charge carries are holes (h^\cdot) obviously. By using Kroger–Vink defect notations, formation of charge carriers can be expressed as follows:



When Fe^{3+} in LaFeO_3 is replaced by Zn^{2+} , the carrier concentration would depend on the holes produced by the ionization of $[\text{Zn}_{\text{Fe}}^x]$:



In this formula, Zn_{Fe}^x means a point defect produced when a Zn^{2+} occupies the sites of a Fe^{3+} ion in the crystal [16]. Upon the addition of Zn^{2+} , holes (h^\cdot) will be generated based on this equation. As a result of $[\text{Zn}_{\text{Fe}}^x] \gg [\text{V}_{\text{La}}^x]$, the concentration of h^\cdot increases, which results in the conductivity of Zn-doping samples considerably higher than that of LaFeO_3 [17].

Gas sensitivity properties of $\text{LaFe}_{1-x}\text{Zn}_x\text{O}_3$

Figure 5 illustrates the influence of the Zn content on the sensitivity of $\text{LaFe}_{1-x}\text{Zn}_x\text{O}_3$ to 100 ppm HCHO. The sensitivity increases with increasing the Zn content up to $x = 0.23$, where it reaches its highest value, and then decreases. The highest sensitivity of the $\text{LaFe}_{1-x}\text{Zn}_x\text{O}_3$ sensor to HCHO is 44.5 with $x = 0.23$. So, much attention was paid to the sensor of $x = 0.23$ in the following.

Figure 6 shows the sensitivity of $\text{LaFe}_{0.77}\text{Zn}_{0.23}\text{O}_3$ to different concentrations of HCHO. It is obvious that the response rise with increasing the gas concentration. Moreover the sensitivity of 500 ppm HCHO reached 188.6.

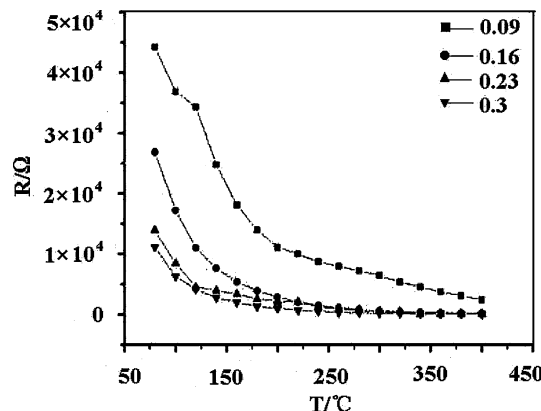


Fig. 4 The resistance-temperature curve of $\text{LaFe}_{1-x}\text{Zn}_x\text{O}_3$ with $x = 0.09, 0.16, 0.23$ and 0.3

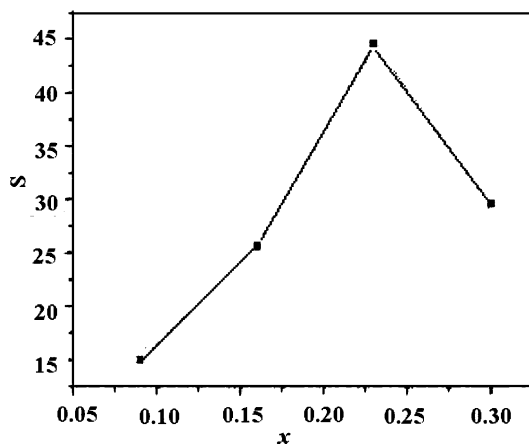
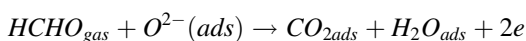


Fig. 5 Influence of x value on the sensitivity of $\text{LaFe}_{1-x}\text{Zn}_x\text{O}_3$ to 100 ppm HCHO

The sensors take on characters of the p-type semiconductor whose conductivity depended on holes when the sensors exposed to the air, O_2 adsorbed on $\text{LaFe}_{1-x}\text{Zn}_x\text{O}_3$ surface would trap electrons from the body of $\text{LaFe}_{1-x}\text{Zn}_x\text{O}_3$ due to the strong electronegativity of the oxygen atom and produced adsorbed oxygen. So the concentration of holes in valence band increases and the resistance of material decreases due to the increasing concentration of available carrier. When reducing HCHO gas is introduced, a chemical reaction happened between HCHO and adsorbed oxygen:



Electrons released from the reaction would annihilate the holes. Hence, the resistance of material increased and conductivity decreases. This suggests that $\text{LaFe}_{1-x}\text{Zn}_x\text{O}_3$ sensors are applicable for detecting HCHO gas.

Furthermore, we measured its selectivity to different gases. From Fig. 7 we can see that the sensitivity of the

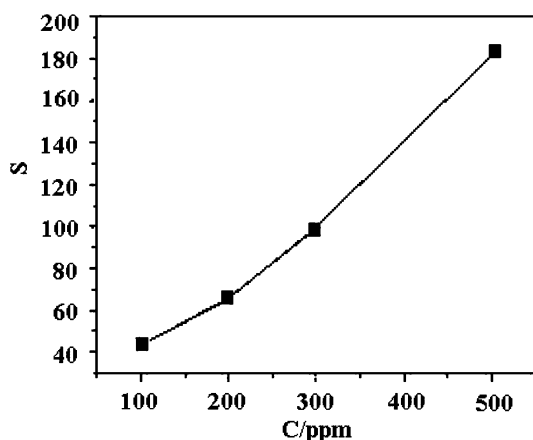


Fig. 6 The sensitivity versus HCHO concentration of $\text{LaFe}_{0.77}\text{Zn}_{0.23}\text{O}_3$ sample

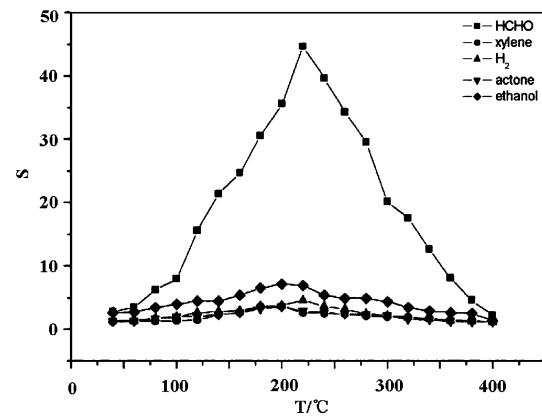


Fig. 7 The selectivity of $\text{LaFe}_{0.77}\text{Zn}_{0.23}\text{O}_3$ -based gas sensor to different gases versus temperature. The gas concentration is 100 ppm

$\text{LaFe}_{0.77}\text{Zn}_{0.23}\text{O}_3$ -based sensor to 100 ppm HCHO is higher than that to 100 ppm acetone, xylylene and H_2 , the result shows that $\text{LaFe}_{0.77}\text{Zn}_{0.23}\text{O}_3$ -based sensor has good selectivity to HCHO.

Response and recovery characteristics are another important properties of gas sensors. Figure 8 shows the response and recovery curve of $\text{LaFe}_{0.77}\text{Zn}_{0.23}\text{O}_3$ when exposed to 100 ppm HCHO at 240 °C. The response curve confirms the p-type semiconductive nature of this material as HCHO is a reducing gas. When HCHO gas was introduced, the resistance of the sensor obviously increased, and the response time t was 25 s. One also can see that after the HCHO gas was removed, the resistance gradually decreased, the recovery time was 50 s.

Conclusions

To conclude, in this paper we have reported for the first time the Zn dopant of $\text{LaFe}_{1-x}\text{Zn}_x\text{O}_3$ with the orthorhombic

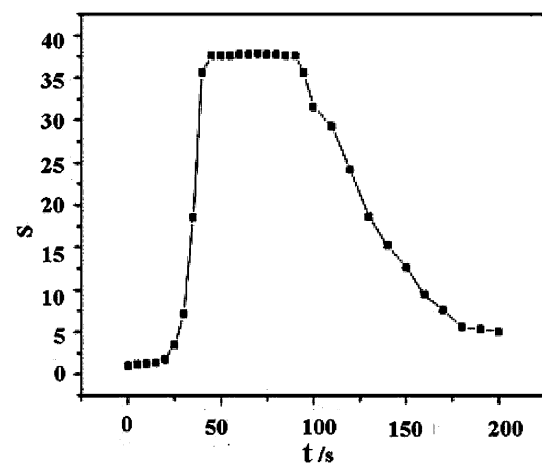


Fig. 8 The response and recovery time characteristics of $\text{LaFe}_{0.77}\text{Zn}_{0.23}\text{O}_3$ -based gas sensor. The gas concentration is 100 ppm

structure synthesized by sol–gel method. This material shows a good response towards HCHO; from measurements at different temperatures and HCHO-amounts we can say that the optimal operation temperature, which meets the requirements of a fast and easily measurable resistance variation, has been found to be around 240 °C.

Among $\text{LaFe}_{1-x}\text{Zn}_x\text{O}_3$ system, the $\text{LaFe}_{0.77}\text{Zn}_{0.23}\text{O}_3$ -based gas sensor shows higher sensitivity to HCHO, and the sensitivity to 100 ppm HCHO is 44.5, to 500 ppm HCHO is 188.6. The $\text{LaFe}_{0.77}\text{Zn}_{0.23}\text{O}_3$ -based gas sensor exhibits short response and recovery times to HCHO, these results point to a possibility to use $\text{LaFe}_{0.77}\text{Zn}_{0.23}\text{O}_3$ -based sensor for monitoring HCHO.

Acknowledgement This work was supported by the National Natural Science Foundation of China.

References

1. Kim WJ, Terada N, Nomura T, Takahashi R, Lee SD, Park JH, Konno A (2002). *Clin Exp All* 32:287
2. Lisi L, Bagnasco G, Ciambelli P (1999). *J Solid State Chem* 146:176
3. Chiu CM, Chang YH (1999). *Thin Solid Films* 342:15
4. Peng ZY, Li X, Zhao MY et al (1996) *Thin Solid Films* 286:270
5. Chiu CM, Chang YH (1999) *Mater Sci Eng A* 266:93
6. Chiu CM, Chang YH (1999) *Sens Actuators B* 54:236
7. Toan NN, Saukko S, Lantto V (2003) *Physica B* 327:279
8. Kong LB, Shen YS (1996) *Sens Actuators B* 30:217
9. Wang YD, Chen JB, Wu XH (2001) *Mater Lett* 49:361
10. Tomoda M, Okano S, Itagaki Y (2004) *Sens Actuators B* 97:190
11. Mantzavinos D, Hartley A, Metcalfe IS (2000). *Solid State Ionics* 134:103
12. Aono H, Traversa E, Sakamoto M (2003). *Sens Actuators B* 94:132
13. Suo H, Wang J, Wu F (1997) *J Solid State Chem* 130:152
14. Song P, Hu J, Qin H (et al) (2004) *Mater Lett* 58:2610
15. Chai YL, Ray DT, Chen GJ, Chang YH (2002) *J Alloys Comp* 333:147
16. Song P, Qin H, Zhang L, An K, Lin Z, Hu J, Jiang M (2005). *Sens Actuators B* 104 :312
17. Kiveer PS (1978) *Physics of semiconductor*, vol 1. English translation, Mir Publishers, p 32
18. Zhang L, Hu JF, Song P et al (2005) *Phys B* 370:259